

# Fast and Accurate Cascaded Particle Swarm Gradient Optimization Method for Solving 2-D Inverse Scattering Problems

M. Farmahini-Farahani, R. Faraji-Dana, and M. Shahabadi

Center of Excellence on Applied Electromagnetic Systems, School of Electrical & Computer Engineering, University of Tehran, P.O. Box 14395-515, Tehran, Iran  
(m.farmahini@ece.ut.ac.ir, reza@ut.ac.ir, shahabad@ut.ac.ir)

**Abstract** – In this paper, a fast and accurate technique for solving the inverse scattering problem of two-dimensional objects made of perfect conductor is proposed. In this technique which is called cascaded particle swarm gradient, the solving procedure is properly divided into two steps. In the first step, the position and the equivalent radius of the unknown objects is estimated while in the second step, the accurate shape function of the objects is determined. The former step is performed by a global optimizer namely particle swarm optimization (PSO) technique and the latter is carried out by the well-known gradient method. In this work, the forward scattering problem is solved by the equivalent source method. Several numerical examples are presented to examine the proposed algorithm especially in handling the challenging multi-object problems with concave shape functions in the presence of measurement errors. The results show that the proposed algorithm is about 75 times faster than a conventional PSO while yielding a higher accuracy.

**Keywords:** Cascaded particle swarm gradient, inverse scattering, and equivalent source method.

## I. INTRODUCTION

Inverse scattering problem generally deals with the extraction of some features of inaccessible objects from the field scattered by them. The information of interest usually includes the shape and material characteristics of the unknown objects. Inverse scattering has many important applications in remote sensing, medical and seismic imaging, non-destructive testing, etc.

The electromagnetic inverse scattering problem is inherently ill-posed and non-linear [1, 2]. A large number of inversion techniques have been developed to solve a variety of electromagnetic inverse scattering problems. While One-dimensional (1-D) problems are more of theoretical importance, two-dimensional (2-D) problems are more realistic and can widely be utilized in practice. It can also be extended to the general case of three-dimensional problems. Here, a 2-D inverse problem for

perfectly conducting objects will be investigated.

Reconstruction algorithms are categorized into two main classes of analytical and numerical. The numerical reconstruction algorithms can be formulated as an optimization problem. Therefore, they can be solved using either global or local optimizers. The majority of proposed numerical inversion algorithms utilize local optimization methods. Some of the well-known methods of this class are the Newton-Kantorovitch method [3], Born iterative method [4], the distorted Born iterative method [5], the local shape function [6] and the conjugate gradient method [7]. However, all of the above mentioned inversion algorithms utilize deterministic optimization methods (DOMs) which are based on the gradient concept. The DOMs generally need an appropriate starting point and a well-behaved cost function to find the global extremum although this is not always guaranteed in practice. Due to these limitations, new global inversion algorithms based on global optimizers are proposed. Global optimization methods, including neural networks, simulated annealing, genetic algorithm (GA), and particle swarm optimization are generally based on evolutionary strategies. These optimization methods have numerous advantages such as implementation simplicity and robustness with respect to initial conditions. However, they generally demand a large number of cost function evaluations, which is always time consuming. It is believed that combined approaches which appropriately benefit from both kinds of optimizers and/or adapt themselves to the nature of the problem would perform more efficiently. For instance, in [8], the cost function evaluation part of the PSO is replaced by a gradient optimizer to achieve a faster convergence. Moreover, [9] has presented a combination of various evolutionary strategies and quasi-deterministic optimizers for efficient optimizing of frequency selective surfaces.

In [10], the inverse problem of a 2-D conductor is solved using *a priori* knowledge of the conductor shape as an initial guess for the gradient optimizer while in [11], GA as a global optimizer is utilized to solve the same problem. Considering the nature of this problem, namely

the fact that it can be divided into two steps of finding a preliminary approximation and extracting exact features, it seems likely that a hybrid method which appropriately combines local and global optimizers can adapt itself to the problem more efficiently.

In this paper, because of some similarity between the scattered fields of the unknown object and those of a circular cylinder of an equivalent radius, we first estimate the position and the approximate radius of the unknown object. Obviously, this searching process must be implemented by a global optimizer. In the next step, a local optimizer uses the initial position and radius obtained by the global optimizer and generates the exact shape profile. Here, PSO is used as a global optimizer. Afterwards, a well-known quasi-Newton method called BFGS (Broyden-Fletcher-Goldfarb-Shanno) [12, 13] is used as a local optimizer.

The paper is organized as follows: In Section II, the formulations of forward and inverse problems are briefly presented and then the inverse problem is formulated as a minimization problem. In Section III, the proposed cascaded PSO-Gradient algorithm is demonstrated. Section IV presents numerical results for single and multiple-object inverse problems with concave profiles and noisy scattered information.

## II. FORMULATION OF THE PROBLEM

The geometry of a typical 2-D inverse problem is depicted in Fig. 1. A perfect cylindrical conductor is placed in free space along the  $z$ -axis and a set of receivers are placed on a surrounding circle. The parametric shape function for the object can be described in a local polar form as,

$$\rho_b' = \rho_b'(\varphi), \quad 0 \leq \varphi \leq 2\pi, \quad O' = \rho_0 \angle \varphi_0, \quad \rho_b = \rho_b' + \rho_0, \quad (1)$$

where the subscript  $b$  stands for boundary and  $O'$  is the origin of a local coordinate system in which the shape function is described. An electromagnetic plane wave with  $E_z$  component is incident upon the cylinder at the incident angle  $\varphi_{inc}$ . Assuming the time harmonic function of  $e^{j\omega t}$ , we express the incident wave by,

$$\mathbf{E}^{inc}(x, y) = E_z^{inc}(x, y) \hat{\mathbf{z}} = e^{jk_0(x \cos \varphi_{inc} + y \sin \varphi_{inc})} \hat{\mathbf{z}} \quad (2)$$

where  $k_0$  is the wave number in free space. Since the incident wave can only produce a  $z$ -directed surface electric current,  $J_z^s$ , one can obtain the integral equation relating the incident field to the induced current on the conductor by applying the PEC boundary condition at the surface of the cylinder, i.e.,  $E_z^t = E_z^s + E_z^{inc} = 0$ . Although

the Method of Moments (MoM) is the prominent numerical technique for solving this type of problems, [14] gives an easier and faster method to find the scattered field based on the equivalent source concept. In this method, the perfectly conducting cylinder is replaced by a set of longitudinal fictitious electric current filaments parallel to the  $z$ -axis which are properly positioned inside the contour  $C$ .

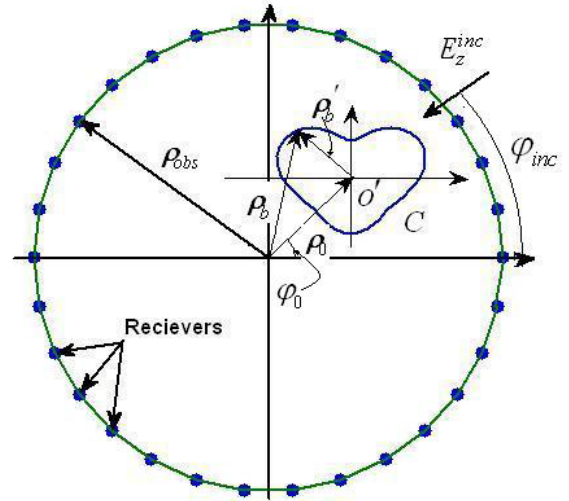


Fig. 1. Geometry of the problem.

According to the equivalence theorem if the electric field produced by these currents satisfies boundary conditions of the perfect conductor object, then the scattered field from the conductor object is equal to the electric field produced by the currents. The total electric field radiated by the currents is given by,

$$E_z(\rho) = -\sum_{m=1}^{N_I} \frac{k_0 \eta}{4} I_m H_0^{(2)}(k_0 |\rho - \rho_m^s|) \quad (3)$$

where the superscript  $s$  in  $\rho_m^s$  stands for source,  $\eta$  is the free space intrinsic impedance,  $N_I$  is the number of current filaments,  $H_0^{(2)}$  is the Hankel function of second kind and zero order and  $I_m$  and  $\rho_m^s$  represent the magnitude and position vector of the current  $m$ -th filament, respectively. To solve the forward problem, it is enough to fulfill PEC boundary condition on the cylinder boundary by equating the total radiated electric field from current filaments of equation (3) and the incident electric field of equation (2) to zero on the surface of the perfect conductor. By selecting  $N_I$  points on the boundary ( $\rho_m^b$ ) and satisfying the boundary condition for these points, which is equivalent to the point-matching technique in MoM, a set of  $N_I$  linear equations is obtained for the

unknown current filaments. Having access to the forward scattering problem solution, one can also solve the inverse problem. In this problem, the object shape function and its associated current filaments must be found such that the radiated electric field becomes the same as the electric field measured at the observation points. The deviation from this ideal case can be measured by using a mean square error criterion defined as,

$$e = \sum_{m=1}^{N_{obs}} \left| E_{meas}^{obs}(\rho_m^{obs}) - E_I^{obs}(\rho_m^{obs}) \right|^2 \quad (4)$$

where the superscript "obs" stands for the observation,  $N_{obs}$  is the number of the observation points,  $\rho_m^{obs}$  is the position vector of the  $m$ -th observation point,  $E_{meas}^{obs}$  is the measured electric field and  $E_I^{obs}$  is the electric field radiated by equivalent current filaments at the observation points. Cumulative error  $e$  must be minimized to yield a satisfactory object reconstruction.

To complete the formulation, one should represent the shape function of the object in a parametric form. Reference [11] suggests a parametric polar form in a local coordinate system, i.e.,

$$\rho(\varphi) = \sum_{n=0}^{N_c/2} a_n \cos(n\varphi) + \sum_{n=1}^{N_c/2} b_n \sin(n\varphi), \quad O' = \rho_0 \angle \varphi_0 \quad (5)$$

where  $N_c$  is the number of trigonometric terms in the approximate series. In this way, the cost function  $e$  is represented as a function of a vector of parameters. This vector,  $X$  can be presented for shape function (5) as,

$$X = [a_0, a_1, \dots, a_{N_c/2}, b_1, b_2, \dots, b_{N_c/2}, \rho_0, \varphi_0]. \quad (6)$$

Therefore, the total number of parameters in equation (6) becomes  $N = N_c + 3$ . The procedure described above can easily be extended to a multi-illumination case where there exists more than one incident electric field. It can also be modified for scattering of multiple objects [10, 11].

### III. CASCADED PARTICLE SWARM-GRADIENT OPTIMIZATION

It is clear that  $e$  is a function of the profile of the cylinder, so the inverse scattering problem is reduced to the strategy of finding a proper shape profile ( $X$  vector) that minimizes  $e$ . In this paper, a novel cascaded strategy provides the proper  $X$  in two steps. In the first step, a

rough approximation of the shape function is acquired using PSO and in the second step the gradient optimizer provides the exact shape using the rough approximation.

It is expected that the scattered field of the unknown cylindrical object and a circular cylinder have the maximum similarity when the circular cylinder is placed in the position of the unknown object and have a proper equivalent radius. This can be explained with the help of an example. Fig. 2 depicts an arbitrary shape function given by  $\rho(\varphi) = 0.3 + 0.05 \cos(2\varphi) + 0.08 \sin(3\varphi)$  placed in  $0.5 \angle 0^\circ$  and its equivalent circular cylinder with the same center and equivalent radius. The incident electric field is located at  $\varphi_{inc} = 0$ . The magnitude of the scattered field of the original object and that of its equivalent circular cylinder sampled on a circle with a radius of 2 wavelengths are plotted in Fig. 3. The similarity between the two scattered fields is obvious. However, it does not necessarily mean that there is no other circular cylinder leading to a smaller error. In general, increasing the number of incident fields will significantly improve the convergence.

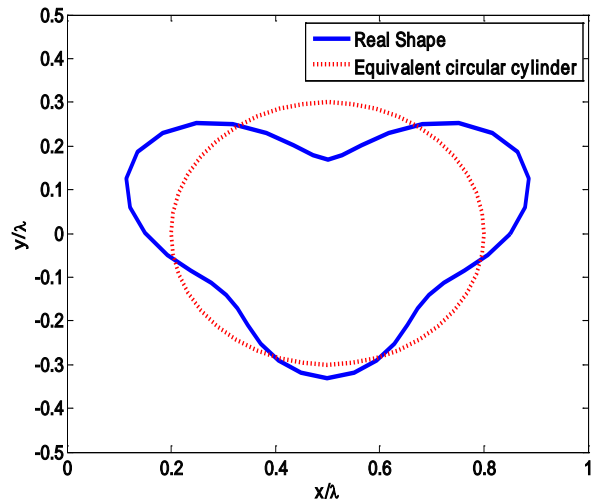


Fig. 2. Arbitrary shape function and its equivalent circular cylinder.

Hence, an initial approximation of the position and the shape of the unknown scatterer can be found by moving the center of a circular cylinder having a variable radius in the search space and comparing the calculated scattered field with the measured scattered field of the unknown object. This searching step is implemented using PSO which is considered as a global optimizer. PSO is a multi-agent stochastic algorithm that emulates food searching process of natural swarms. PSO has a conceptually simple and sensible algorithm based on

Newtonian concept of position and velocity. A detailed description of this technique can be found in [15, 16].

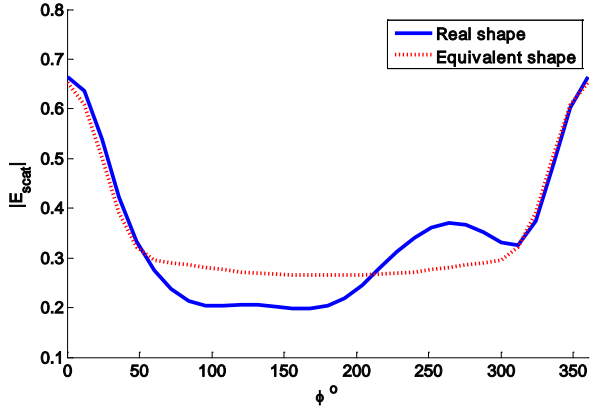


Fig. 3. Absolute value of scattered fields for Fig. 2 objects.

In the first step of the proposed cascaded algorithm, the optimization parameter vector is defined as follows,

$$X = [r_0^{(1)}, r_0^{(2)}, \dots, r_0^{(N_o)}, \rho_0^{(1)}, \rho_0^{(2)}, \dots, \rho_0^{(N_o)}, \varphi_0^{(1)}, \varphi_0^{(2)}, \dots, \varphi_0^{(N_o)}] \quad (7)$$

where  $r_0^{(n)}$ ,  $\rho_0^{(n)}$  and  $\varphi_0^{(n)}$  are the equivalent radius and the polar coordinate components of the  $n$ -th unknown object, respectively. Then the values of  $a_0^{(n)}$ ,  $\rho_0^{(n)}$ , and  $\varphi_0^{(n)}$  in equation (6) are replaced by  $r_0^{(n)}$ ,  $\rho_0^{(n)}$ , and  $\varphi_0^{(n)}$  respectively, while other parameters are set to zero. In the next step, the initial position and radius of the object serves as an appropriate initial guess for a gradient based optimizer [10]. The well-known quasi-Newton method, BFGS, is adopted for this stage to yield accurate shape functions.

After evaluating the performance of individual parts of algorithm, they are unified to establish a cascaded operation which we have named as cascaded *particle swarm gradient method*.

#### IV. NUMERICAL RESULTS AND DISCUSSION

To examine the proposed method and to show its accuracy and convergence, several numerical experiments have been performed. The following mean square error function has been defined to quantitatively measure the accuracy of the shape functions,

$$SE = \left[ \frac{1}{N_I N_o} \sum_{n=1}^{N_o} \sum_{m=1}^{N_I} \frac{(\rho_{n,m}^{opt} - \rho_{n,m}^{true})^2}{(\rho_{n,m}^{true})^2} \right]^{1/2} \quad (8)$$

In all these experiments, the dimensions are normalized to the wavelength and the observation points are placed on a circle with a radius equal to 2 wavelengths. In addition,  $N_{obs}, N_I, N_c$  are set to 30, 20 and 6, respectively. The search ranges for  $r_0, \rho_0, \varphi_0$  are whit in  $0.1 \leq r_0 \leq 1, 0 \leq \rho_0 \leq 1.5$  and  $0 \leq \varphi_0 \leq 360^\circ$ . SNR and PSO iterations are also selected to be 20dB and 200, respectively. As a first example, the shape function used in [11] is selected. The shape profile is given by  $\rho(\varphi) = 0.3 + 0.05 \sin(2\varphi)$  in local polar coordinate whose center is placed at  $0.5 \angle 90^\circ$ . Moreover, two incident electric fields are assumed with incidence angles equal to 0 and  $\pi$ . Additive white Gaussian noise (AWGN) is added to the measured data with SNR=20dB. In [11], a real coded genetic algorithm is proposed for the profile reconstruction of the 2-D conducting objects. It optimizes the whole  $X$  vector, namely 9 parameters in this case, simultaneously. In our method, however there are only 3 parameters for position and equivalent radius to be optimized using a global optimizer in the first step and 7 parameters for coefficients of the shape function in equation (6) in the second step. PSO converged after 200 iterations to the values  $\rho_0 = 0.4987, \varphi_0 = 89.96^\circ, r_0 = 0.3040$ , and BFGS started with these initial values as initial and converged after 13 iterations.

Besides, a simple PSO code is utilized to solve the same problem. It should be mentioned that the range of variables in (6) is defined in such a way that both methods search over the same area. Figure 4 shows the true profile, the equivalent circular cylinder found by PSO, the final PSO-BFGS reconstructed profile and the simple PSO reconstructed one. Figure 5 shows the convergence of cascaded PSO-gradient for the shape of Fig. 5 compared with the ordinary PSO.

While the cascaded PSO-BFGS solves the problem in just 12 seconds with  $SE=1.6\%$  it takes 15 minutes for the ordinary PSO to converge with  $SE=3\%$ . This indeed shows the superiority of the proposed method over an ordinary PSO. PSO-BFGS is about 75 times faster than the ordinary PSO and provides a slightly better accuracy in this particular example. To examine robustness of the algorithm against noise, the above example is solved for various amounts of added noise. Figure 6 shows the  $SE$  versus SNR. Achieving a  $SE$  of 10.12% at SNR=2.5dB demonstrates the excellent noise immunity of the proposed technique.

As the second example, two objects of shape functions  $\rho(\varphi) = 0.3 + 0.05 \sin(3\varphi)$  and  $\rho(\varphi) = 0.3 + 0.05 \sin(2\varphi)$  are selected and placed at  $0.5 \angle 90^\circ$  and  $0.5 \angle 270^\circ$  locations, respectively. The existence of two objects with concave shapes makes this example more challenging compared to the previous one.

Again two angles of incidence namely zero and  $\pi$  are selected. The SNR of the measured data was set to 20dB. After 750 iterations, the first step of the algorithm converged to values of  $r_0^{(1)} = 0.307, \rho_0^{(1)} = 0.513, \varphi_0^{(1)} = 89.7^\circ$  for the upper object and  $r_0^{(2)} = 0.306, \rho_0^{(2)} = 0.497, \varphi_0^{(2)} = 269.7^\circ$  lower one.

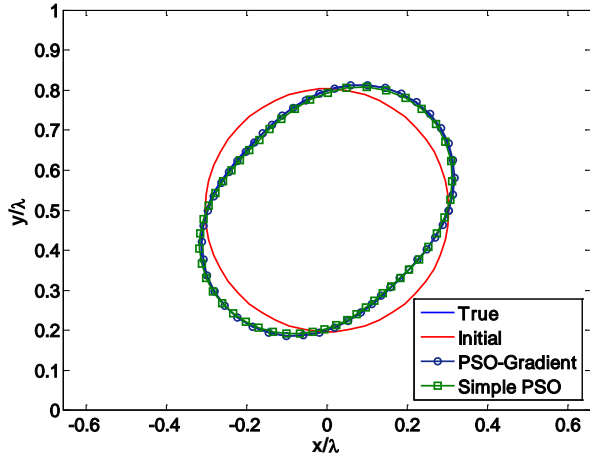


Fig. 4. True, initial guess, and reconstructed profile with PSO-BFGS and ordinary PSO.

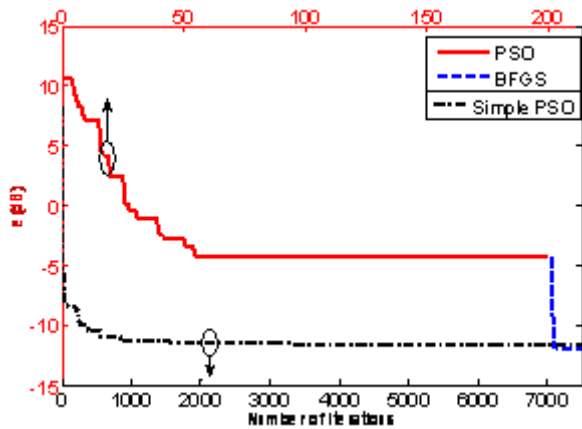


Fig. 5. Convergence of the cascaded PSO-BFGS compared with an ordinary PSO for the reconstruction of the shape function of Fig. 4.

These values were used as the initial guess for the gradient algorithm which converged after 19 iterations. Figure 7 shows the true profiles, the equivalent circular cylinders found by PSO, and the final reconstructed profiles. Figure 8 presents the cost function variations during cascaded PSO-BFGS iterations. Clearly, the proposed method can effectively solve the inverse problem in the case of multi-scatterers. The total computation time for achieving SE=6.05% is less than two minutes on a P4-3.2 GHz PC. It should be noted that the deviation observed at the bottom of the upper object is due to the multi-scattering effect.

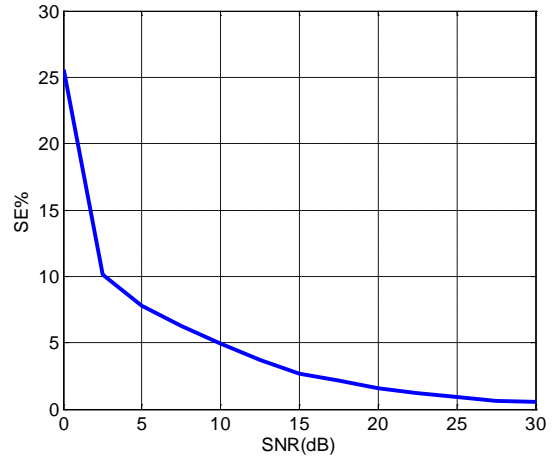


Fig. 6. Variations of SE versus SNR.

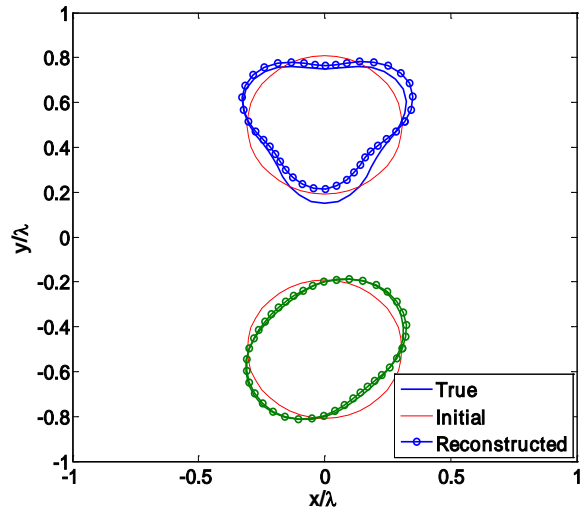


Fig. 7. True, initial, and reconstructed profiles of two scatterers using cascaded PSO BFGS.

To investigate the performance of the two parts of the algorithm against concavity, a statistical experiment is carried out. The ratio of  $a_n/a_0$  or  $b_n/a_0$  can be changed to obtain a variety of profiles with different concavities. Different values of  $a_2/a_0$  and  $b_3/a_0$  can produce three types of profiles, namely elliptical, tri-lobe and their combination. The PSO part is operated 1000 times for different profiles of each type. For each type, the most concaved shape profile for which the performance of the PSO part is still acceptable and the obtained equivalent circle is depicted in Table. 1. The percentage of PSO failed hits, denoted by the *FP* parameter, demonstrates the performance of PSO in finding the equivalent circle for each profile. The *FP* values presented in the table.1 demonstrates the satisfactory performance of the PSO part in finding a proper initial guess even for very concave shape functions.

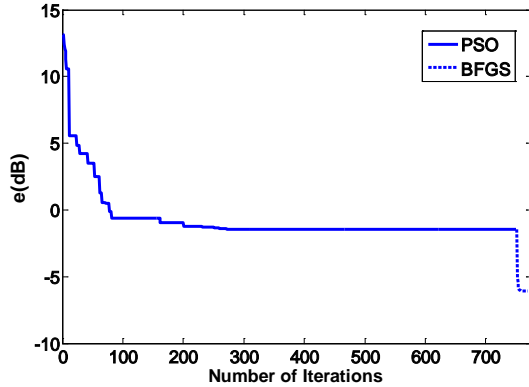

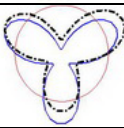



Fig. 8. Convergence of the proposed method in reconstruction of the profiles of Fig. 7.

It is important to address the performance of the Gradient part against concavity of the shape profile. To do this, the initial circles from Table. 1 are used in the BFGS algorithm as the starting point and the final shape functions are obtained. The obtained shape functions from gradient part are also depicted in Table. 1 (thick dashed lines) and the corresponding shape errors (SE) are also presented. Unsurprisingly, the gradient part fails to give an accurate shape function for the tri-lobe profile; however, the result is still similar to the original shape. A quasi-gradient approach to address this problem is now under investigation.

Furthermore, the angle of incidence is an important issue in multi-objects cases. For instance, the algorithm will fail if we set the incident angles around  $\pi/2$  or  $3\pi/2$  in the second example. The numerical results indicate that the suitable combination of the global and local optimization techniques as achieved in the proposed method has improved the accuracy and reduced the computation time significantly while avoiding the well-known disadvantages of both techniques.

Table 1. Obtained shape functions from gradient part.

	$\frac{a_2}{a_0}$	$\frac{b_3}{a_0}$	Profile	FP(%)	SE(%)
3	0.2	0		11.9	6
8	0	0.75		12.8	32.3
10	0.25	0.25		8.5	23.3
True shape function (thick solid line) corresponding equivalent circle (thin solid line) Estimated shape function (thick dashed line)					

## V. CONCLUSION

In this paper, a cascaded PSO gradient optimization method suitable for solving the inverse scattering problem of 2-D perfect conductors is presented. The versatility of the proposed method is shown by applying it to challenging case of multi-objects with concave shapes and noisy data. The numerical results show satisfactory performance of the proposed method considering the important criteria of computation time and the achieved accuracy.

## REFERENCES

- [1] A. J. Devancy, "Nonuniqueness in the inverse scattering problem," *J.Math. Phys.*, vol. 19, no. 7, pp. 1526–1531, 1978.
- [2] M. Bertero and C. De Mol, "Stability problems in inverse diffractions," *IEEE Trans. Antennas Propagat.*, vol. AP-29, no. 2, pp. 368–372, 1981.
- [3] A. Roger, "Newton–Kantorovitch algorithm applied to electromagnetic inverse problem," *IEEE Trans. Antennas Propagat.*, vol. AP-29, pp. 232–238, 1981.
- [4] M. Moghaddam and W. C. Chew, "Nonlinear two-dimensional velocity profile inversion using Time-domain data," *IEEE Trans. Geosci. Remote* vol. 30, pp. 147–156, Jan. 1992.
- [5] W. C. Chew and Y. M. Wang, "Reconstruction of two-dimensional permittivity using the distorted Born iterative method," *IEEE Trans. Med. Imag.*, vol. 9, pp. 218–225, 1990.
- [6] W. C. Chew and G. P. Otto, "Microwave imaging of multiple conducting cylinders using local shape functions," *IEEE Microwave Guided Wave Lett.*, vol. 2, pp. 284–286, July 1992.
- [7] R. V. McGahan and R. E. Kleinman, "Image reconstruction using real data," *IEEE Trans. on Antennas and Propagation*, vol. 38, pp. 39–59, Mar. 1996.
- [8] M. Ghaffari-Miab, M. Ghaffari-Miab, A. Farmahini-Farahani, R. Faraji-Dana, and C. Lucas, "An efficient hybrid swarm intelligence-gradient optimization method for complex time Green's functions of multilayer media," *Progress In Electromagnetics Research*, PIER 77, 181–192, 2007.
- [9] A. Fallahi, M. Mishrikey, C. Hafner, and R. Vahldieck, "Efficient procedures for the optimization of frequency selective surfaces," *IEEE Trans. on Antennas and Propagation*, vol. 56, no. 5, pp. 1340–1349, May 2008.
- [10] C. Y. Lin and Y. W. Kiang, "Inverse scattering for conductors by the equivalent source method," *IEEE Trans. on Antennas and Propagation*, vol. AP-44 pp. 310–315.

- [11] A. Qing, C. K. Lee, and L. Jen, "Electromagnetic inverse scattering of two-dimensional perfectly conducting objects by real coded genetic algorithm," *IEEE Trans. Geosci. Remote Sensing*, vol. 39, pp. 665-676, Mar. 2001.
- [12] D. Goldfarb, "A family of variable metric updates derived by variational means," *Mathematics of Computing*, vol. 24, pp. 23-26, 1970.
- [13] Fletcher, R., "A new approach to variable metric algorithms," *Computer Journal*, vol. 13, pp. 317-322, 1970.
- [14] A. Kirsch, R. Kress, P. Monk, and A. Zinn, "Two methods for solving the inverse acoustic scattering problem," *Inverse Problems*, vol. 4, pp. 749-770, 1988.
- [15] J. Robinson and Y. Rahma-Samii, "Particle swarm optimization in electromagnetics," *IEEE Trans. on Antennas and Propagation*, vol. 52, no. 2, pp. 397-408, Feb. 2004.
- [16] N. Jin and Y. Rahmat-Samii, "Advances in particle swarm optimization for antenna design: real number, binary, single-objective and multi-objective implementations," *IEEE Trans. on Antennas and Propagation*, vol. 55, no. 3, pp. 556-567, Mar. 2007.



research interests are inverse scattering, spatial power combining and optimization methods in Electromagnetics.

**Mohsen Farmahini Farahani** received the B.Sc. from Iran University of Science and Technology (with honors) in electrical engineering in 2006 and M.Sc. degree from the University of Tehran in 2009, both in electrical engineering. He is currently a research associate with the School of Electrical and Computer Engineering, University of Tehran. His



1994, he joined the School of Electrical and Computer Engineering, University of Tehran, where he is currently a Professor. He has been engaged in several academic and executive responsibilities, among which was his deanship of the Faculty of Engineering for more than four years, up until summer 2002, when he was elected as the University President

**Reza Faraji-Dana** received the B.Sc. degree (with honors) from the University of Tehran, Tehran, Iran, in 1986 and the M.A.Sc. and Ph.D. degrees from the University of Waterloo, Waterloo, ON, Canada, in 1989 and 1993, respectively, all in electrical engineering.

He was a Postdoctoral Fellow with the University of Waterloo for one year. In

by the university council. He was the President of the University of Tehran until December 2005. He is the author of several technical papers published in reputable international journals and refereed conference proceedings.

Prof. Faraji-Dana has been the Chairman of the IEEE-Iran Section since March 2007. He received the Institution of Electrical Engineers Marconi Premium Award in 1995.



**Mahmoud Shahabadi** received the B.Sc. and M.Sc. degrees from the University of Tehran, Iran, and the Ph.D degree from Technische Universitaet Hamburg-Harburg, Germany, all in electrical engineering in 1988, 1991, and 1998, respectively. In 1998, he joined the School of Electrical and Computer Engineering, University of Tehran, where he is currently an Associate

Professor. From 2001 to 2004, he was with the Department of Electrical and Computer Engineering, University of Waterloo, Canada, as a Visiting Professor. Additionally he is a co-founder and CTO of MASSolutions Inc., a Waterloo-based company with a focus on advanced low-profile antenna array systems. His research interests and activities encompass various areas of microwave and millimeter-wave engineering as well as photonics. Computational electromagnetics for microwave engineering and photonics find his special interest. He is currently conducting research and industrial projects in the field of antenna engineering, photonic crystals, left-handed materials, and holography. Dr. Shahabadi was awarded the 1998/1999 Prize of the German Metal and Electrical Industries, Nordmetall, for his contribution to the field of millimeterwave holography.